Use of diabatic basis in the adiabatic-by-sector R-matrix propagation method in time-independent reactive scattering calculations

ARTICLE *in* COMPUTER PHYSICS COMMUNICATIONS · NOVEMBER 2001

Impact Factor: 3.11 · DOI: 10.1016/S0010-4655(01)00287-9

1 AUTHOR:

Hiroki Nakamura
National Chiao Tung University
238 PUBLICATIONS **4,102** CITATIONS

Computer Physics Communications 140 (2001) 381–398

Computer Physics Communications

www.elsevier.com/locate/cpc

Use of diabatic basis in the adiabatic-by-sector R-matrix propagation method in time-independent reactive scattering calculations

Gennady V. Mil'nikov [a,b], Hiroki Nakamura [a,*]

[a] *Division of Theoretical Studies, Institute for Molecular Science, Myodaiji, Okazaki 444-8585, Japan*
[b] *Permanent address: Institute of Structural macrokinetics, Russian Academy of Sciences, Chernogolovka, Moscow region 142432, Russia*

Received 22 June 2000; received in revised form 5 March 2001; accepted 6 April 2001

Abstract

We propose a new recipe for the *R*-matrix propagation which combines the ideas of the adiabatic-by-sector (ABS) method and the sequential diagonalization/truncation technique. The *R*-matrix is determined in the adiabatic representation but the method does not require calculations of adiabatic channel functions at radial points inside the sector of propagation. This is a modification of the previously proposed ABS approach and can significantly reduce the computational time and memory in the energy independent part of scattering calculations. The code is checked by a test calculation of the reaction $O(^3P) + HCl \rightarrow OH + Cl$ using a LEPS potential energy surface (PES). The applicability of the method is further demonstrated by accurate quantum calculations of the endoergic reaction $H(^2S) + O_2(^3\Sigma_g^-) \rightarrow OH(^2\Pi) + O(^3P)$.

PACS: 03.65.Nk; 11.55.-m; 34.10.+x

Keywords: R-matrix propagation; Diabatic basis; Variational

1. Introduction

In this paper we present a modification of the numerical method for time-independent scattering calculations proposed by Tolstikhin and Nakamura [1], which is based on the adiabatic-by-sector approach with use of the SDT (sequential diagonalization/truncation) technique [1] and is supposed to be more efficient than the ordinary DBS (diabatic-by-sector) method. Although the method is quite general, we restrict our attention to tri-atomic systems with zero total angular momentum quantum number and consider the Schrödinger equation in the hyperspherical coordinates (ρ, ω),

$$\left[K(\rho) + H_{ad}(\omega; \rho) - \mu\rho^2 E\right]\Psi(\rho, \omega) = 0. \tag{1}$$

* Corresponding author.
E-mail address: nakamura@ims.ac.jp (H. Nakamura).

[1] The essentially the same idea as the SVD (slow/smooth variable discretization) method proposed in [2] and used in [1] had actually been considered previously by Light and Bacic [3].

0010-4655/01/$ – see front matter
PII: S0010-4655(01)00287-9

Here

$$K(\rho) = -\frac{1}{2}\frac{\partial}{\partial\rho}\rho^2\frac{\partial}{\partial\rho} + \frac{15}{8} \tag{2}$$

represents the hyperradial kinetic energy and the adiabatic Hamiltonian $H_{ad}(\omega;\rho)$ depends on ρ as a parameter. The general strategy in solving Eq. (1) is to expand $\Psi(\rho,\omega)$ in terms of some functions in hyperangle variables ω. A possible choice for this basis is a set of adiabatic channel functions $\Phi_\nu(\omega;\rho)$ which, at each ρ, are the eigenfunctions for the adiabatic Hamiltonian

$$\left[H_{ad}(\omega;\rho) - \mu\rho^2 U_\nu(\rho)\right]\Phi_\nu(\omega;\rho) = 0. \tag{3}$$

Such a direct expansion, however, leads to undesirable numerical difficulties related with nonsmooth behaviour of the nonadiabatic coupling terms. The diabatic-by-sector (DBS) method [4] is much more handy and it has been commonly used in chemical reaction computations. The whole interval of the hyperradius ρ ("scattering" coordinate) is divided into a number of sectors and, within a sector, a single set of diabatic basis functions is used. This leads to the familiar close coupling (CC) equations for the radial components which can be solved by various methods [5]. At the boundaries between sectors the transformation to the new diabatic basis is to be done in order to preserve the continuity of the total wave function and its derivative. It is worth to note that the diabatic and adiabatic approaches are not identical as long as one has to truncate the expansion by a finite number N_{ch} of propagated channels. In particular the CC equations of the DBS method are equivalent to those in adiabatic treatment only up to an extra term which does not vanish even for arbitrarily small sector size [6]. It has been found in the study of dt μ problem that this discrepancy may cause poor convergence of the DBS method at low collision energies [7].

In the numerical scheme recently suggested by Tolstikhin and Nakamura (TN) [1] the R-matrix $\mathcal{R}_{\nu\mu}(\rho)$ is defined in terms of the adiabatic channel functions $\Phi_\nu(\omega;\rho)$ but the adiabatic CC equations are not solved. Instead, for each sector the radial motion is represented by the DVR method and the R-matrix is propagated by the technique of Ref. [8] in combination with the sequential diagonalization/truncation (SDT) approach [3,9]. The initial condition for the propagation is guaranteed by the appropriate choice of the DVR functions in the first sector and the propagation reduces to a few algebraic operations with some auxiliary matrices calculated in the spectral representation. The method requires no matching at the boundaries between sectors and all the computations are carried out essentially by a variational method which guarantees rapid convergence and the better accuracy of the results as was demonstrated by several examples [1,10,11]. Eq. (3), however, must be solved at each DVR radial point and this is where most of the computational effort in energy-independent part is involved. For more complicated systems the number of locally open adiabatic channels grows and this computation appears to be still expensive in the TN code. In the present work we modify the method in order to avoid the calculation of the adiabatic channel functions at the DVR quadrature points inside sectors and reduce the computational task.

2. Modification of the TN method

We first outline the basic equations of the TN approach [1]. The R-matrix $\mathcal{R}_{\nu\mu}(\rho)$ is defined in terms of the adiabatic surface functions as

$$\left\langle \Phi_\nu(\omega;\rho) \mid \Psi(\rho,\omega)\right\rangle = \mathcal{R}_{\nu\mu}(\rho)\left\langle \Phi_\mu(\omega;\rho) \,\middle|\, \frac{\partial}{\partial\rho}\Psi(\rho,\omega)\right\rangle. \tag{4}$$

It satisfies zero boundary conditions at the origin and must be propagated up to asymptotically large ρ_f where the scattering data is extracted. In practice the zero boundary conditions are imposed at some small $\rho_0 > 0$. The whole interval of the propagation is divided into sectors and the numerical task is to calculate $\mathcal{R}(\tilde{\rho}_k)$ at the right end $\tilde{\rho}_k$ of the kth sector $[\tilde{\rho}_{k-1}, \tilde{\rho}_k]$, if $\mathcal{R}(\tilde{\rho}_{k-1})$ at the left end is known. In order to do this we first consider the sector eigenvalue problem,

$$\left[\widetilde{K}(\rho) + H_{ad}(\omega;\rho) - \rho^2 E_n\right]\Psi_n(\rho,\omega) = 0; \quad \rho \in \left[\tilde{\rho}_{k-1}, \tilde{\rho}_k\right], \tag{5}$$

where $\widetilde{K}(\rho)$ is the symmetrized kinetic energy operator [8]. The sector eigenfunctions Ψ_n are found in the form of the expansion

$$\Psi_n(\rho,\omega) = \sum_{i=1}^{N_\rho}\sum_{\nu=1}^{N_{ch}} C_{i\nu}^n \pi_i(\rho)\Phi_\nu(\omega;\rho_i), \tag{6}$$

where N_ρ is the number of DVR quadrature points ρ_i inside the sector and $\pi_i(\rho)$ are the corresponding DVR basis functions. $\pi_i(\rho)$ for the first sector are constructed from Jacobi polynomials $P_n^{(0,2)}$ which give linear behaviour $\sim(\rho-\rho_0)$ of the wave function at $\rho\sim\rho_0$, and the Legendre polynomials are used for all the other sectors. The propagation of the R-matrix is carried out according to the relation [8,12],

$$\mathcal{R}(\rho_k) = R^{(k,k)} - R^{(k,k-1)}\left[R^{(k-1,k-1)} + \mathcal{R}(\rho_{k-1})\right]^{-1} R^{(k-1,k)}, \tag{7}$$

where the auxiliary matrices $R_{\nu\mu}^{(k,l)}$ are defined by

$$R_{\nu\mu}^{(k,l)} = \frac{\tilde{\rho}_k\tilde{\rho}_l}{2}\sum_n \frac{\langle\Phi_\nu(\omega;\tilde{\rho}_k) \mid \Psi_n(\tilde{\rho}_k,\omega)\rangle\langle\Phi_\mu(\omega;\tilde{\rho}_l) \mid \Psi_n(\tilde{\rho}_l,\omega)\rangle}{(E_n - E)}. \tag{8}$$

Here $\langle\,|\,\rangle$ stands for the 2D integral on the hypershere and the summation is over all the $N_\rho \times N_{ch}$ eigenvalues E_n. The expansion Eq. (6) implies that the channel functions $\Phi_\nu(\omega;\rho_i)$ must be calculated at each of N_ρ DVR points inside the sector. In the TN approach this is the most time consuming part of the calculations [1,10,11]. Thus it would be desirable not to repeat the solution of Eq. (3) N_ρ times for each sector. This can be achieved by using the same adiabatic basis for neighboring points ρ_i.[2] Since in any case the R-matrix requires the computation of the surface functions $\Phi_\nu(\omega;\tilde{\rho}_k)$ at the boundaries $\tilde{\rho}_k$ of sectors, it is natural to use them as much as possible. Thus we take N_ρ to be an even number and modify the expansion Eq. (6) as follows

$$\Psi^n(\rho,\omega) = \sum_{i=1}^{\frac{N_\rho}{2}}\sum_{\nu=1}^{N_d} C_{i\nu}^n \pi_i(\rho)\Phi_\nu\left(\omega;\tilde{\rho}_{k-1}\right) + \sum_{i=\frac{N_\rho}{2}+1}^{N_\rho}\sum_{\nu=1}^{N_d} C_{i\nu}^n \pi_i(\rho)\Phi_\nu\left(\omega;\tilde{\rho}_k\right). \tag{9}$$

In other words, $\Phi_\nu(\omega;\tilde{\rho}_k)$ are used as the diabatic basis for the "right half" of the kth sector and for the "left half" of the $(k+1)$th sector. This simply corresponds to the substitution of the adiabatic channel functions $\Psi_\nu(\omega,\rho_i)$ in the expansion Eq. (6) by $\Psi_\nu(\omega,\hat{\rho}_i)$ with the representative points $\hat{\rho}$,

$$\hat{\rho}_i = \tilde{\rho}_{k-1} \quad \text{for } i = 1,\ldots,\frac{N_\rho}{2}, \tag{10}$$

$$\hat{\rho}_i = \tilde{\rho}_k \quad \text{for } i = \frac{N_\rho}{2}+1,\ldots,N_\rho. \tag{11}$$

We have also introduced the number of "diabatic" functions N_d which generally does not need to coincide with the number of the propagated channels N_{ch}. Inserting Eq. (9) to Eq. (5), we arrive at the $N_\rho \times N_d$-dimensional eigenvalue problem for the coefficients $C_{i\nu}^n$,

$$\sum_{j=1}^{N_\rho}\sum_{\mu=1}^{N_d}\left(\widetilde{K}_{ij}\,\widehat{O}_{i\nu,j\mu} + \mu\left[\hat{\rho}_i^2 U_\nu(\hat{\rho}_i) - \rho_i^2 E_n\right]\delta_{ij}\delta_{\nu\mu} + \left[H_{ad}(\omega;\rho_i) - H_{ad}(\omega;\hat{\rho}_i)\right]_{\nu\mu}\delta_{ij}\right)C_{j\mu}^n = 0, \tag{12}$$

[2] The similar idea has been previously implemented by Choi and Light [13] for calculating the spectrum of H_2O.

where the matrix elements of $\widetilde{K}$ is given by

$$\widetilde{K}_{ij} = \frac{1}{2}\int_{\tilde{\rho}_{k-1}}^{\tilde{\rho}_k} \frac{\mathrm{d}\pi_i(\rho)}{\mathrm{d}\rho}\rho^2\frac{\mathrm{d}\pi_j(\rho)}{\mathrm{d}\rho}\,\mathrm{d}\rho + \frac{15}{8}\delta_{ij} \tag{13}$$

and $\widehat{O}_{iv,j\mu}$ is the overlap matrix

$$O_{iv,j\mu} = \big\langle \Phi_v(\omega;\hat{\rho}_i) \mid \Phi_\mu(\omega;\hat{\rho}_j)\big\rangle. \tag{14}$$

For both i and j within the same "half"of the sector, $[1,\ldots,\frac{N_\rho}{2}]$ or $[\frac{N_\rho}{2}+1,\ldots,N_\rho]$, the overlap matrix is simply reduced to $\delta_{ij}\delta_{v\mu}$. Otherwise the elements of $\widehat{O}_{iv,j\mu}$ are determined as $\langle\Phi_v(\omega;\tilde{\rho}_{k-1}) \mid \Phi_\mu(\omega;\tilde{\rho}_k)\rangle$. Note also that the last term in Eq. (12) actually contains only the matrix elements of the potential $\mu[\rho_i^2 V(\rho_i,\omega) - \hat{\rho}_i^2 V(\hat{\rho}_i,\omega)]$ which is easy to be computed. Eqs. (9) and (12) together with Eqs. (7) and (8) constitute the basic equations of our new recipe for the R-matrix propagation.

A question which still needs to be clarified concerns the number and the accuracy of the adiabatic channel functions $\Phi_\mu(\omega;\tilde{\rho}_k)$ which are used now in two different ways. First, they appear in the definition and the propagation recipe for the R-matrix. The required dimension N_{ch} of the R-matrix is determined by the number of locally open channels and depends on the energy interval. This dictates the choice of numerical parameters for solving the adiabatic eigenvalue problem Eq. (3), since at the boundaries of sectors we need at least N_{ch} accurate surface functions.

In addition to this, $\Phi_v(\omega;\tilde{\rho}_k)$ are used as the diabatic basis in Eq. (9) for the DVR points inside sectors. Obviously, the higher the dimension N_d of the diabatic basis is, the better result for the sector R-matrices is obtained. In our calculations we have actually found that the accuracy of the final scattering data is greatly improved by a moderate increase of N_d, even if the highest $N_d - N_{ch}$ adiabatic channels are not well converged ones. This is explained by the fact that Eq. (8) for the auxiliary sector matrices can be obtained by the same variational method as for the elements of the resolvent operator. To see this we consider the following functional:

$$I_{v\mu}^{(kl)}(\chi,\hat{\chi}) = \big\langle \Phi_v(\omega;\tilde{\rho}_k) \mid \hat{\chi}(\tilde{\rho}_k,\omega)\big\rangle + \big\langle \Phi_\mu(\omega;\tilde{\rho}_l) \mid \chi(\tilde{\rho}_l,\omega)\big\rangle + \big\langle \chi\big|\rho^2 E - \mathcal{H}\big|\hat{\chi}\big\rangle_{3\mathrm{D}}, \tag{15}$$

where $\mathcal{H}$ is the sector Hamiltonian in Eq. (5) and the last matrix element is understood as the 3D integral. $I_{v\mu}^{(k,l)}(\chi,\hat{\chi})$ is a variational functional for $R_{v\mu}^{(k,l)}$, when we take $\chi(\rho,\omega)$ and $\hat{\chi}(\rho,\omega)$ as independent trial functions. Indeed it is easy to show that

$$R_{v\mu}^{(k,l} = I_{v\mu}^{(kl)}\big(\chi_0,\hat{\chi}_0\big), \tag{16}$$

where $\chi_0(\rho,\omega)$, $\hat{\chi}_0(\rho,\omega)$ satisfy the variational principle

$$\delta I_{v\mu}^{k,l}(\chi,\hat{\chi}) = 0. \tag{17}$$

$I_{v\mu}^{k,l}(\chi,\hat{\chi})$ is very similar to the functional which appears as a variational expression for the generic matrix elements of the resolvent operator [14,15]. As it has been shown by Miller and Jansen [15], this allows to express the matrix element in terms of arbitrary set of trial function u_s. In the present case the analogous result is written as

$$R_{v\mu}^{(k,l)} = \frac{\tilde{\rho}_k\tilde{\rho}_l}{2}\sum_{s,s'}\big\langle \Phi_v(\omega;\tilde{\rho}_k) \mid u_s(\tilde{\rho}_k,\omega)\big\rangle\big(\big\langle u_s\big|\mathcal{H}-\rho^2E\big|u_{s'}\big\rangle_{3\mathrm{D}}\big)^{-1}\big\langle u_{s'}(\tilde{\rho}_l,\omega) \mid \Phi_\mu(\omega;\tilde{\rho}_l)\big\rangle, \tag{18}$$

where $(\langle u_s|\mathcal{H}-\rho^2E|u_{s'}\rangle_{3\mathrm{D}})^{-1}$ denotes the s,s' element of the inverse of the matrix $\langle u_s|\mathcal{H}-\rho^2E|u_{s'}\rangle_{3\mathrm{D}}$. Eq. (18) is equivalent to Eq. (8), if we choose the trial functions as

$$u_s \equiv u_{i,v} = \pi_i(\rho)\Phi_v\big(\omega;\hat{\rho}_i\big). \tag{19}$$

Indeed, the set of the sector eigenfunctions Ψ_n is obtained by a rotation of the basis $\{u_s\}$ which enables us to avoid the numerical inversion of the matrix $\langle u_s|\mathcal{H}-\rho^2E|u_{s'}\rangle$. The trial functions u_s need not satisfy any specific

equation and Eq. (18) applies as it is even when u_s are not normalized or not orthogonal [15]. Thus, the accuracy of the highest $N_d - N_{ch}$ surface functions Ψ_ν is not so important, since they appear only as a part of this variational basis.

We summarize now the above discussion and formulate the numerical strategy as follows. We divide the interval of propagation $[\rho_0, \rho_f]$ into N_{sct} sectors and solve the adiabatic eigenvalue problem Eq. (3) at the boundaries of sectors $\tilde{\rho}_k,\ k = 0, 1, \ldots, N_{sct},\ \rho_{N_{sct}} = \rho_f$. The numerical parameters should be chosen in order to get N_{ch} accurate adiabatic channel functions, where N_{ch} is the dimension of the R-matrix to be propagated. At every $\tilde{\rho}_k$ we also store the extra $N_d - N_{ch}$ adiabatic channel functions in order to increase, if necessary, the diabatic basis which is used for calculating $R^{(kl)}_{\nu\mu}$. The accuracy of these extra functions is not important. For every sector all the matrix elements $\langle \Phi_\nu(\omega; \tilde{\rho}_k) \mid \Psi_n(\tilde{\rho}_k, \omega)\rangle$ are calculated and stored together with E_n. This ends the energy independent part of the calculation. The R-matrix is then propagated at various energies according to Eq. (7) which can be effectively done by using the Nesbet algorithm [16]. The cpu time of the energy dependent part is mostly determined by the evaluation of sector R-matrices (Eq. (8)) which is linear with N_d. At the same time a moderate increase of N_d significantly improves the accuracy of S-matrix. For instance, in the scattering calculations for HOCl system given in the next section, two more-digits of accuracy in S-matrix was obtained by increasing the number of the diabatic functions from 130 to 140 which requires only about 10% increase of the cpu time. The last step of the calculations is the matching to the asymptotic states at $\rho = \rho_f$ which does not need any modification and can be found in [1].

3. Numerical illustration

3.1. $O + HCl \to OH + Cl$

We first present results of quantum scattering calculations for the reaction

$$O(^3P) + HCl \to OH + Cl \tag{20}$$

using LEPS PES [17]. This provides a good test for the new recipe since the same system has been studied previously by the TN formalism [1]. Similar to Ref. [1] the adiabatic eigenvalue problem Eq. (3) is solved by the DVR-SDT method using hyperspherical elliptic coordinates ρ, ξ, η [18]. The hyperspherical angle coordinates ξ, η span the range

$$2\gamma < \xi < 2\pi - 2\gamma, \quad -2\gamma < \eta < 2\gamma, \tag{21}$$

where γ is the angle of the Smith kinematic rotation between the two heavy-light arrangements. In this coordinate system Eq. (3) reads

$$K(\eta) + \mu\rho^2\big((\cos\eta - \cos\xi)U_\nu(\rho) - h_{ad}(\xi; \eta, \rho)\big)\Phi_\nu(\xi, \eta; \rho) = 0, \tag{22}$$

where $K(\eta)$ represents the kinetic energy for η-motion and h_{ad} plays a role of the adiabatic 1D Hamiltonian at fixed η and ρ. The explicit form of K and h_{ad} can be found in [1]. For both hyperangles the initial DVR basis $\pi^\eta_i(\eta)$ and $\pi^\xi_i(\xi)$ of corresponding dimensions N_η and N_ξ are constructed from the Legendre polynomials. We first diagonalize $h_{ad}(\xi; \eta_i, \rho)$ at all N_η DVR points η_i. This gives the new basis functions $\phi_{n_\xi}(\xi; \eta_i, \rho)$ as a solution of the eigenvalue problem

$$\big[h^\eta(\xi; \eta_i, \rho) - \mu\rho^2(\cos\eta_i - \cos\xi)\varepsilon_{n_\xi}(\eta_i, \rho)\big]\phi_{n_\xi}(\xi; \eta_i, \rho) = 0. \tag{23}$$

We use n_{ad} functions $\phi_{n_\xi}(\xi; \eta_i, \rho)$ at each DVR point η_i so that the final dimension of the adiabatic eigenvalue problem is $N_\eta \times n_{ad}$. For convenience our notations are summarized in Table 1. The DVR method is very convenient for TN approach, since we need to evaluate $\frac{(N_\rho+1)(N_\rho+2)}{2} - 1$ overlap matrices for each sector. At the same time the method is known to be not very efficient at large ρ where the surface functions are highly localized. For example, in the previous study of HClO system $N_\eta = 150$ was required to represent the highest rotational states in both

Table 1
Notations and parameters of the multidimensional basis

ξ_i, η_i	DVR ponts on the hypershere	
$\tilde{\rho}_k$	Right boundary of the kth sector	
ρ_i	DVR radial points	$\tilde{\rho}_{k-1} < \rho_1 < \rho_2 < \cdots < \rho_{N_\rho} < \tilde{\rho}_k$
N_ξ, N_η	Number of the DVR points ξ_i and η_i	
n_{ad}	Dimension of the truncated 1D basis $\phi_{n_\xi}(\xi;\eta,\rho)$	
N_ρ	Number of the DVR radial point for a sector	
N_{ch}	Dimension of the R-matrix $\mathcal{R}_{v\mu}(\rho)$	
N_d	Dimension of the diabatic basis	

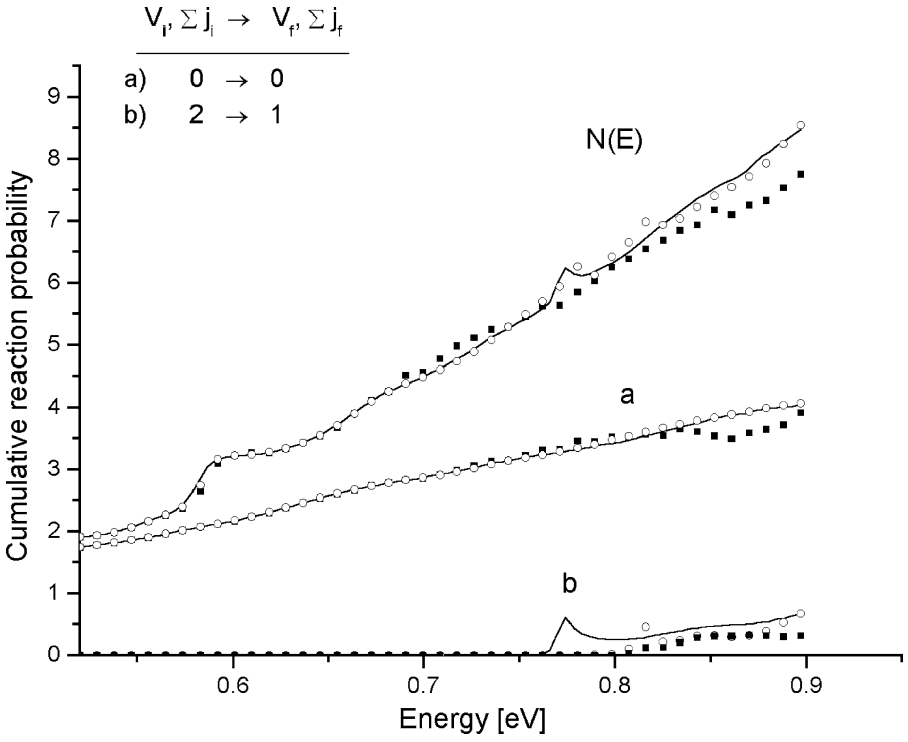

Fig. 1. Cumulative probabilities for the reaction (20) calculated by the present method with the parameters $n_{ad} = 10$, $N_{ch} = N_d = 100$ (squares), $n_{ad} = 12$, $N_{ch} = N_d = 110$ (circles). Solid line represents TN results [1].

arrangements O + HCl and Cl + OH. In turn, one must take at least $n_{ad} = 10$ in order to reproduce the lowest $N_{ch} = 100$ adiabatic radial terms $U_v(\rho)$ with the accuracy better than 1 meV. In the present scheme we need only one diagonalization and one overlap matrix per sector similar to the DBS method. Thus we can easily adjust the initial DVR basis for different ρ as well as use other methods for solving Eq. (3) [19–22]. However, in the present work for the sake of simplicity and for comparison purposes we didn't change this part of the calculations and use the same basis as in Ref. [1]. As a first test, we implement the present approach with the same parameters $N_{ch} = 100$ and $n_{ad} = 10$ without increasing the "diabatic" basis ($N_d = N_{ch}$). The results for various cumulative reaction probabilities are presented in Fig. 1. One can see that without increasing N_d the present approach cannot

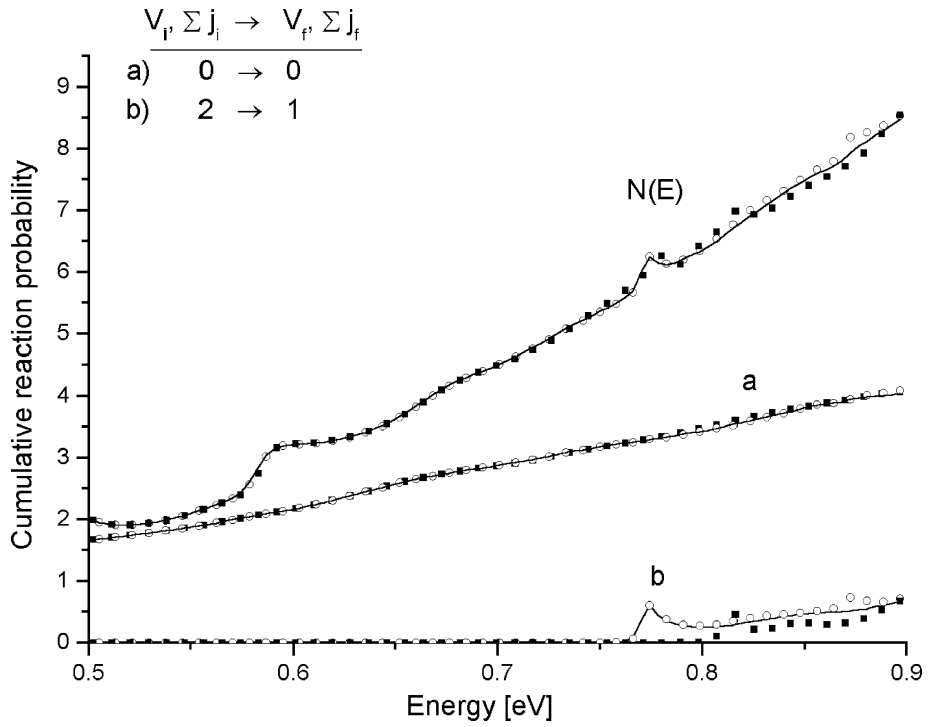

Fig. 2. The same as Fig. 1 except that the numerical parameters are: $n_{ad} = 12$, $N_{ch} = N_d = 110$ (squares), $n_{ad} = 14$, $N_{ch} = N_d = 130$ (circles).

improve the results at energies higher than 0.7 eV. The increase of the number of propagated channels N_{ch} even when the surface functions are calculated accurately at the boundaries of sectors doesn't make the results much better. In the same plot we show the data corresponding to $N_d = N_{ch} = 110$, $n_{ad} = 12$. n_{ad} was increased in order to reach the same accuracy (about 1 meV) for the extra 10 adiabatic channels. Although these results are much better for $E < 0.75$ eV, the discrepancy still persists at higher energies. This is especially manifested in the probability P_{21} for $(v_i = 2,\ \sum j_i) \to (v_f = 1,\ \sum j_f)$. In principle, the results can be improved by further increasing the number of channels (see Fig. 2) but it converges very slowly. As was pointed out above good convergence is easily achieved by increasing the basis for evaluating $R_{v\mu}^{(k,l)}$. Fig. 3 shows the results for larger $N_d = 130$ and $N_d = 140$ with $N_{ch} = 100$, $n_{ad} = 10$, both of which nicely reproduce the previous one. The accuracy of the highest 30 ($= N_d - N_{ch}$) adiabatic channel functions in "diabatic" basis is not high (the error in adiabatic radial terms is larger than 20 meV), but they improve the results very much. At the same time the increase of N_d does not require extra numerical effort in solving the adiabatic channel problem. Thus, for OHCl system the present numerical scheme is about 8 times less expensive than the previous one. Another factor which gives a measure of accuracy is the symmetry of S-matrix. In the case of $N_d = 130$ the symmetry of S-matrix is guaranteed up to 3 significant digits, which is similar to the previous TN results. With $N_d = 140$ it is not worse than 5 digits even at the highest energy considered with only about 10% increase of the cpu time compared to the case $N_d = 130$.

3.2. $H + O_2 \to OH + O$

To further demonstrate the capability of the method we provide accurate 3D quantum calculations for $H + O_2$ combustion reaction,

$$H(^2S) + O_2(^3\Sigma^-) \to OH(^2\Pi) + O(^3P). \tag{24}$$

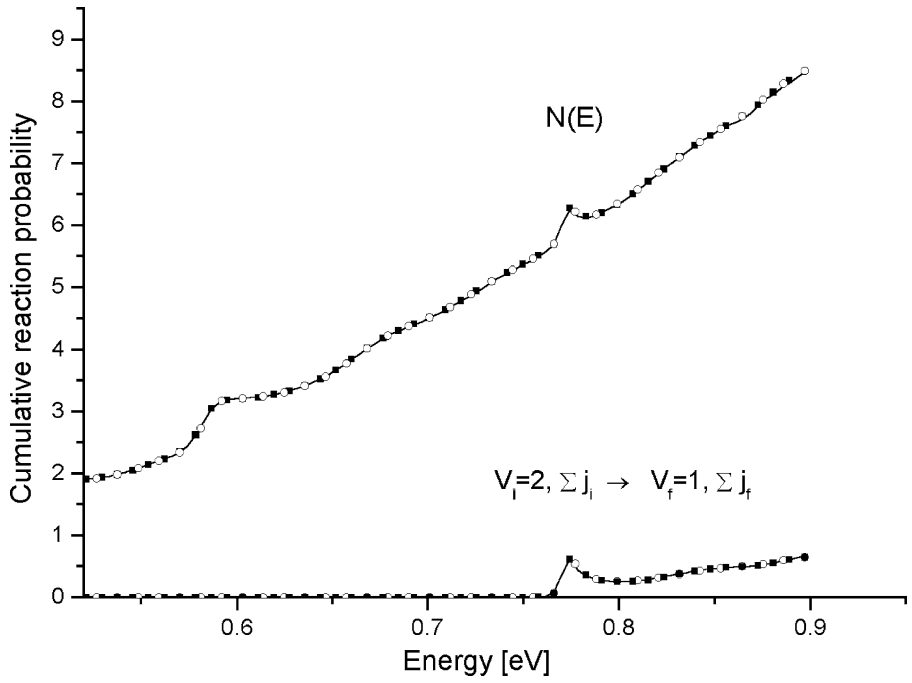

Fig. 3. Cumulative reaction probabilities for the reaction (20) with $n_{ad} = 10$, $N_{ch} = 100$. The dimension of the diabatic basis is $N_d = 130$ (circles) and $N_d = 140$ (squares).

This reaction plays an important role in combustion chemistry and has been extensively studied both theoretically and experimentally [23–31]. The detailed time-independent calculations for the state-to-state reaction probabilities in the framework of the APH hyperspherical coordinate approach were done by Pack et al. [32,33]. There are several reasons which prompted us to consider this system again. The exchange of the hydrogen atom between two oxygen atoms has the HLH mass combination which makes this system attractive to be studied by the hypersherical elliptic coordinates. At the same time its accurate dynamics study is more difficult that the HLH systems treated so far. The reaction complex OOH has a deep potential well which causes a large number of locally open channels at short internuclear distances. Besides, due to the large endoergicity of the reaction there are many O_2 ro-vibration states open before the energy reaches the reaction threshold. The asymptotic area is also characterized by the long range behavior of the potential due to dipole-quadrupole interaction between $O(^3P)$ atom and OH radical. The hyperspherical elliptic coordinates are powerful to elucidate the reaction mechanisms in HLH systems. The vibrationally adiabatic ridge lines can be clearly defined just like in the collinear case [34,35]. Avoided crossings in the vicinity of the ridge lines were shown to play an important role in the reaction dynamics [36]. However, there have been no attempts to elaborate a qualitative concept to explain the role of the condensation region [37] in the reaction mechanism. One could expect that this becomes especially important for systems like HO_2. However, the high density of states and many narrow resonances in the final reaction probabilities make any simple analysis in terms of separate avoided crossings almost impossible. This inspired us to develop a more efficient method for treating them numerically.

We used the DMBE PES [38] which is similar to the one used by Pack et al. [33]. The adiabatic channel functions $\Phi_\nu(\eta, \xi; \rho)$ and energies $U_\nu(\rho)$ were calculated as described above. The behaviour of $U_\nu(\rho)$ is shown on Fig. 4 over the ρ-interval [3.5, 8.5] (in a.u.). The symmetry of the system with respect to the reflection $\eta \to -\eta$ reduces the size of final 2D diagonalization to one-half. Similarly to the previous studies of this reaction we consider only odd functions with respect to O–O exchange which is consistent with the symmetry of the asymptotic $O_2(^3\Sigma_g^-)$.

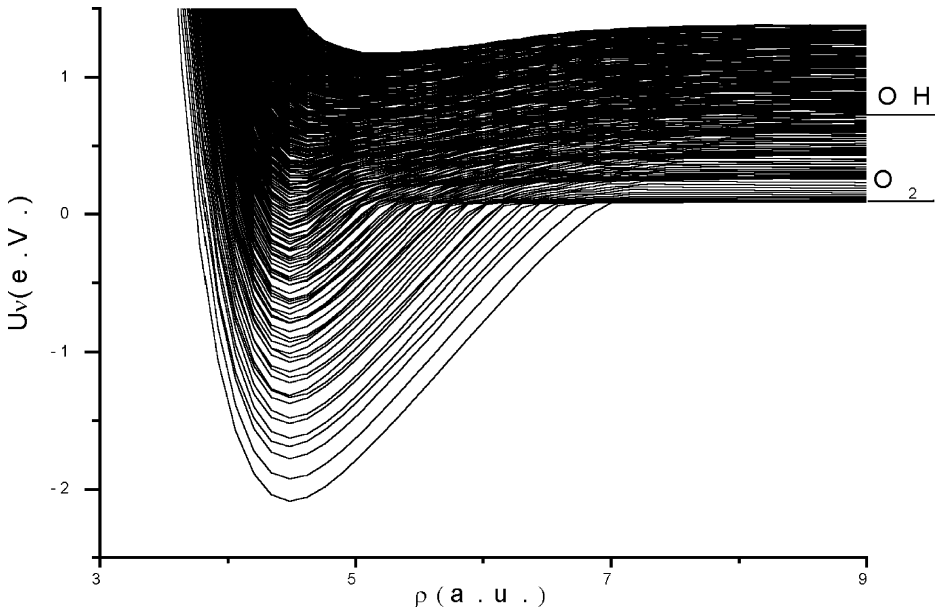

Fig. 4. Adiabatic radial terms for the reaction (24).

Figs. 5 show the behaviour of the potential function in the 2D ξ, η space for three values of the hyperradius $\rho = 4.2, 5.7, 11.2$ (a.u.). The solutions of the internal adiabatic eigenvalue problem ε_{n_ξ} for the same values of ρ are presented in Figs. 6.

In the asymptotic region the potential qualitatively resembles LEPS PES (Fig. 5(a)); but the valley for $H + O_2$ arrangement (located approximately at $(\xi - \pi)/(\pi - 2\gamma) = 0.7$ on Fig. 4(a)) is as deep as those of the arrangement $O + OH$ in the two corners at the bottom of the picture. When ρ increases further, this valley becomes deeper and most of the surface functions in the asymptotic region correspond to the $H + O_2$ reaction channel (see Fig. 4). Rotation of the diatomic fragment O_2 is well reproduced by the η-motion which is almost parallel to the equipotential contours while the ξ-motion represents the vibration. At intermediate ρ the system forms a stable complex and the corresponding contour plot is depicted on Fig. 5(b) ($\rho = 5.7$ a.u.). The O_2 arrangement is still well separated by the potential barrier $\sim$1.6 eV along ξ-coordinate. Two symmetric wells are associated with $O + HO$ arrangements and the motion along η-coordinate represents the exchange of hydrogen between two oxygen atoms. These minima are about 1.2 eV deeper than the very flat valley in the O_2 arrangement and most of the adiabatic channel functions at intermediate ρ are diabatically connected with the asymptotic $O + HO$ channels. It was pointed out [1] that the breakdown of the adiabatic separability between the two elliptic hyperangles mostly occurs at the linear H-L-H configuration which corresponds to $\xi = 2\gamma$ in Figs. 5. In the case of LEPS PESs used before for other reaction systems, this appears as a sharp angle in the equipotential contours at the line $\xi = 2\gamma$ and provides a mechanism for the vibrational excitation in light atom exchange reaction [1,36]. From the numerical point of view this requires to increase the number n_{ad} of internal adiabatic functions. Thus, in the scattering calculations of the reaction (20) considered above, $n_{ad} = 10$ was required to accurately treat the asymptotic states with vibrational quantum numbers $v = 0, 1, 2$ in both arrangements. On the contrary, in the case of HO_2 the linear configuration is almost forbidden energetically and we have the better adiabatic separability. At smaller ρ (Fig. 5(c)) rearrangement processes start to play a role and finally the O_2 and OH arrangements overlap. These features of PES correlate with the behaviour of the internal adiabatic energies in Eq. (23) (Figs. 6). Because of the symmetry of the potential only one half of the η-interval is depicted. The O_2 and OH arrangements at large ρ appear as two clearly distinguishable families of curves and the internal adiabatic functions $\phi_{n_\xi}(\xi; \eta, \rho)$ belonging to different families do not overlap.

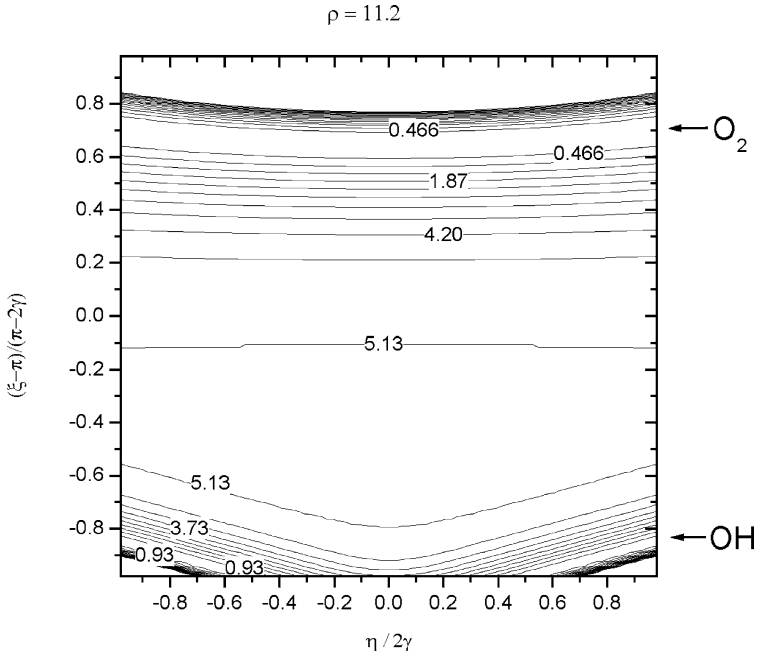

(a)

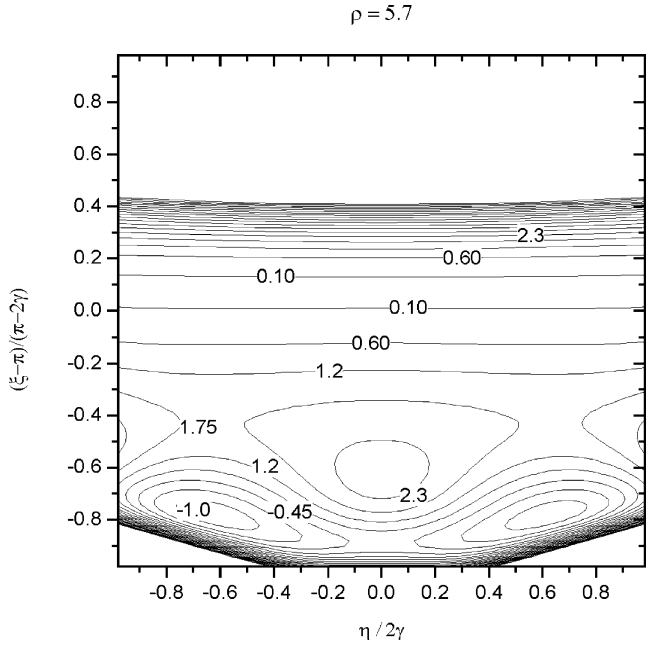

(b)

Fig. 5. Contour plots of the DMBE PES for the reaction (24) in the hyperspherical elliptic coordinates for three representative values of the hyperradius: (a) The asymptotic region ($\rho = 11.2$) where all three arrangements are well separated; (b) intermediate region ($\rho = 5.7$); (c) the condensation region ($\rho = 4.2$), where the HO_2 complex is formed.

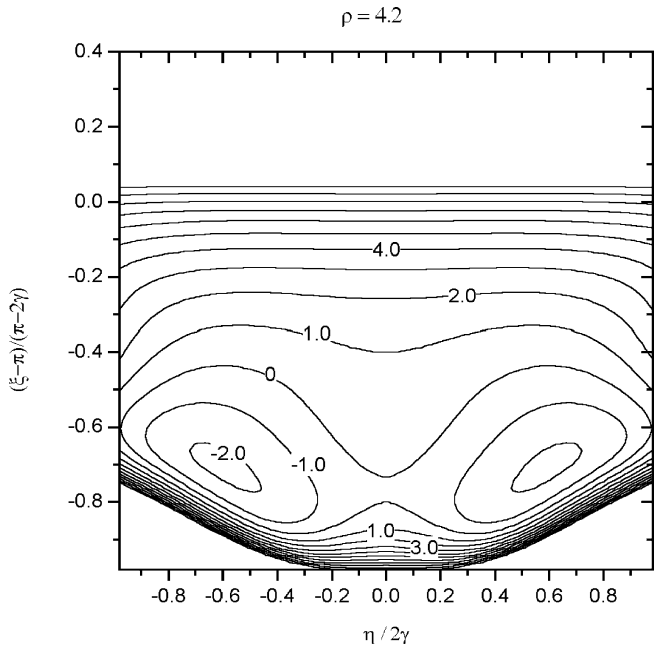

(c)

Fig. 5. (Continued.)

As was mentioned above, the valley in the O_2 arrangements is very weakly dependent on η and the adiabatic curves are almost straight lines, showing a very good separability between the hyperangles. As a result, we can accurately calculate many asymptotic states in this channel with a moderate value of n_{ad}. The accuracy of the asymptotic functions in O + HO channel is generally worse, since in this part DMBE and LEPS PES are qualitatively similar. In the preliminary calculations of the surface functions at large ρ we used $n_{ad} = 15$ which is the total number of curves in Fig. 6(a) below 1.5 eV. Nine of the 15 functions $\phi_{n_\xi}(\xi; \eta, \rho)$ can be "assigned" to the $O_2 + H$ channel and it was enough to reproduce the corresponding radial terms with accuracy better than 10^{-3} meV. At the same time the higher exited states in the HO + O channel still showed bad convergence and we had to increase n_{ad} up to 30 to reach the accuracy of 0.3 meV. When ρ decreases, the O_2 family almost does not change, although the spacing between "straight lines" becomes slightly smaller (see Fig. 6(b)). The second family changes drastically. They shift down and twice as many adiabatic curves appear in the same energy interval compared to Fig 6(a). At this ρ the two families of states are still clearly different and show no conspicuous avoided crossings. Similarly to the asymptotic region, the quality of the adiabatic separability of the hyperangles is different for the two families and the numerical accuracy is better for O_2 family. At the same time the linear HLH configuration is energetically disadvantageous at these ρ and the elliptic coordinates become better also for the OH family. Although the total number of locally open radial terms at intermediate ρ is larger than at asymptotic distances and most of them correspond to the "bad" O + HO configuration, $n_{ad} = 35$ was enough to obtain the same accuracy ($\sim$0.3 eV) for all the channels. Finally Fig. 6(c) shows $\varepsilon_{n_\xi}(\eta, \rho)$ at $\rho = 4.2$ a.u. where the two families completely mix. At short distances like this a single potential valley is formed. The motions perpendicular and parallel to this valley correspond to vibration and rotation of the triatomic system, respectively, and can be approximately represented by the motion along ξ and η coordinates. The separability in this interval is good and $n_{ad} = 30$ is enough to obtain all the adiabatic radial terms with the accuracy 0.1 meV or better. For reactive processes the interval of ρ below $\sim$5.7 a.u. is the important region of configuration space. In particular, the cumulative reaction probability [39–42] can be evaluated without

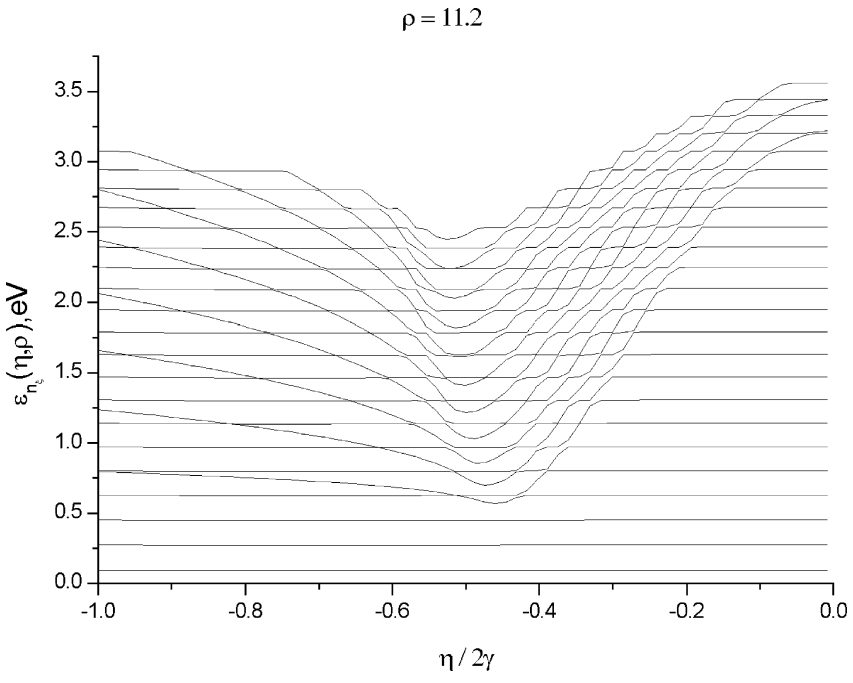

(a)

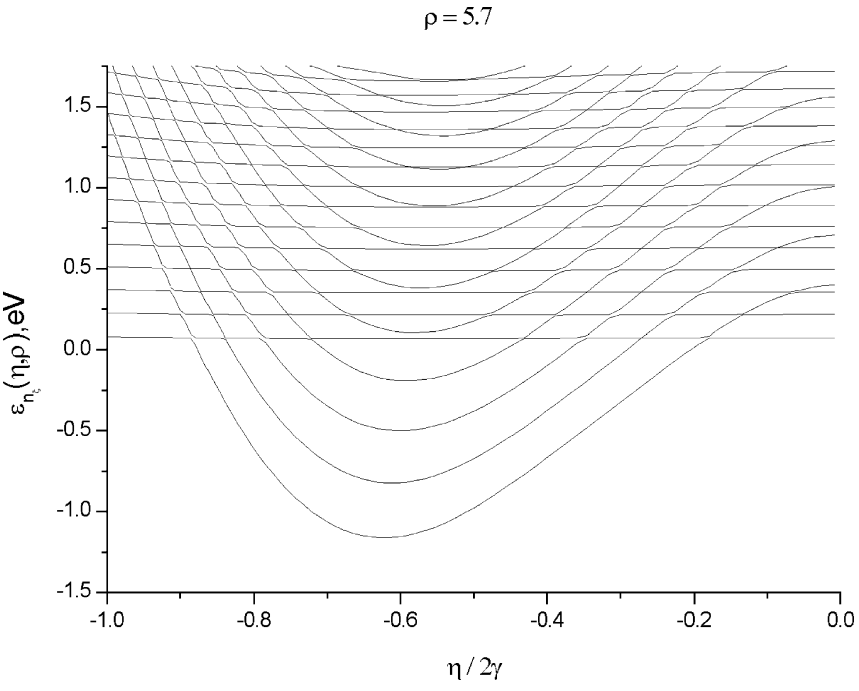

(b)

Fig. 6. Eigenvalues of Eq. (23) at the same three values of ρ as those in Figs. 5.

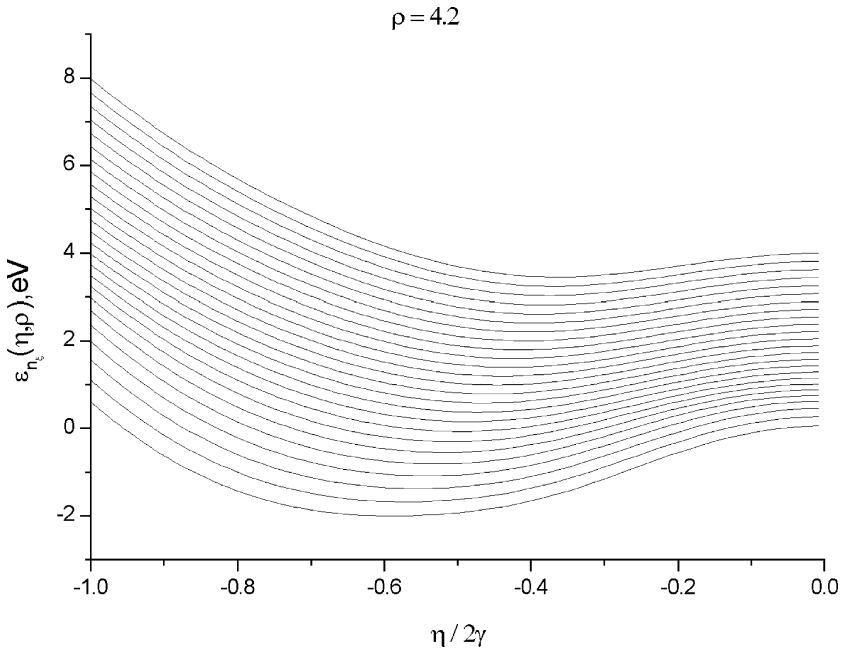

(c)

Fig. 6. (Continued.)

propagating the R-matrix beyond 6 a.u. The full S-matrix naturally requires a much longer propagation which is still feasible in the present scheme.

There is one more difference from the other HLH systems considered before. Due to the deep potential well in the HO_2 complex the number of locally open channels in the asymptotic region is much smaller than that at shorter distances. Thus, it is necessary to change smoothly the dimension of the R-matrix with ρ and avoid the calculations of extra adiabatic functions which are not required at the matching radius. By doing this we can reduce the computer time of the R-matrix propagation which must be repeated at many values of the energy. In the propagation recipe defined by Eqs. (7) and (8) this can be easily carried out. In the definition of the matrices $R_{\nu\mu}^{(k,l)}$ (see Eq. (8)) different number of the adiabatic channels at the left ($N_{ch}^{(k-1)}$) and the right ($N_{ch}^{(k)}$) end of the sector can be considered. In this case, one has generally two square and two rectangular matrices,

$$R_{\nu\mu}^{(k-1,k-1)}, \quad \nu,\mu = 1,2,\ldots,N_{ch}^{(k-1)},$$
$$R_{\nu\mu}^{(k,k)}, \quad \nu,\mu = 1,2,\ldots,N_{ch}^{(k)},$$

and

$$\begin{aligned} &R_{\nu\mu}^{(k-1,k)}, \quad \nu = 1,2,\ldots,N_{ch}^{(k-1)},\ \mu = 1,2,\ldots,N_{ch}^{(k)},\\ &R_{\nu\mu}^{(k,k-1)}, \quad \nu = 1,2,\ldots,N_{ch}^{(k)},\ \mu = 1,2,\ldots,N_{ch}^{(k-1)}. \end{aligned} \tag{25}$$

For $N_{ch}^{(k-1)} \neq N_{ch}^{(k)}$, Eq. (7) is still valid as it is. The dimensions of the diabatic basis in the first and the second sum in the expansion Eq. (9) can also be different. We just need to introduce the corresponding number of functions $N_d^{(k-1)} \neq N_d^{(k)}$ which lead to evident modifications in the sector eigenvalue problem Eq. (12). For the present reaction we propagated the R-matrix of the maximum dimension $N_{ch} = 330$ up to $\rho = 5.7$ a.u. For larger ρ we

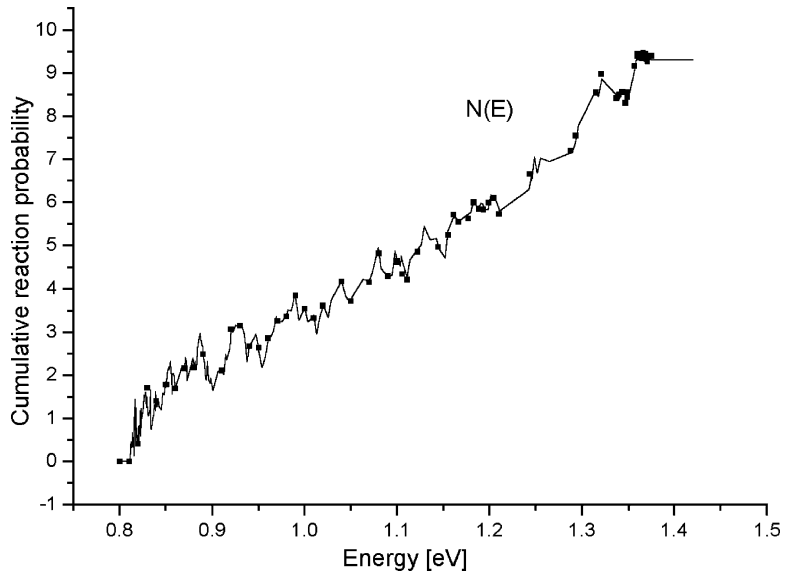

(a)

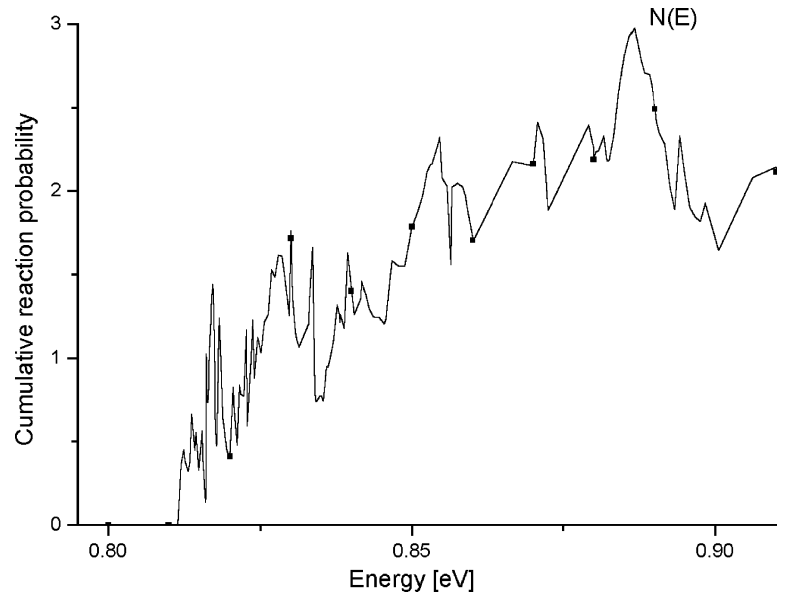

(b)

Fig. 7. Cumulative reaction probability for the reaction (24). (a) Plot over the full energy interval. (b) Blow up of the low energy region to show the resonance structures. The number of the propagated channels N_{ch} are ranged from 330 to 270 (solid lines) and from 350 to 290 (squares).

decreased N_{ch} sector by sector and at the matching radius finally used 270 channels. The number N_d of the diabatic basis function was taken as $N_d^{(k)} = N_{ch}^{(k)} + 50$ at all the points $\tilde{\rho}_k$. We repeated the calculations at $E < 1.1$ eV to check that this $\Delta N = N_d - N_{ch} = 50$ is large enough. The other numerical parameters are: $\rho_0 = 3.2$ a.u., $\rho_f =$

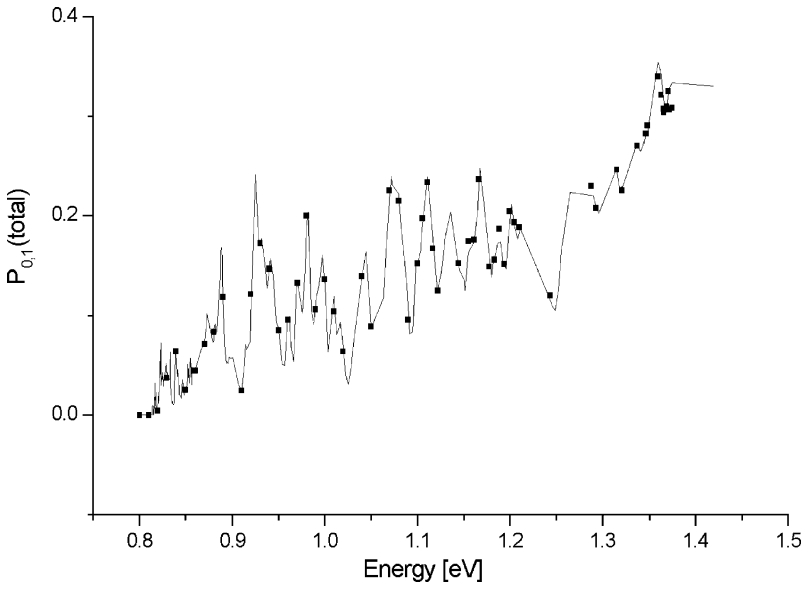

(a)

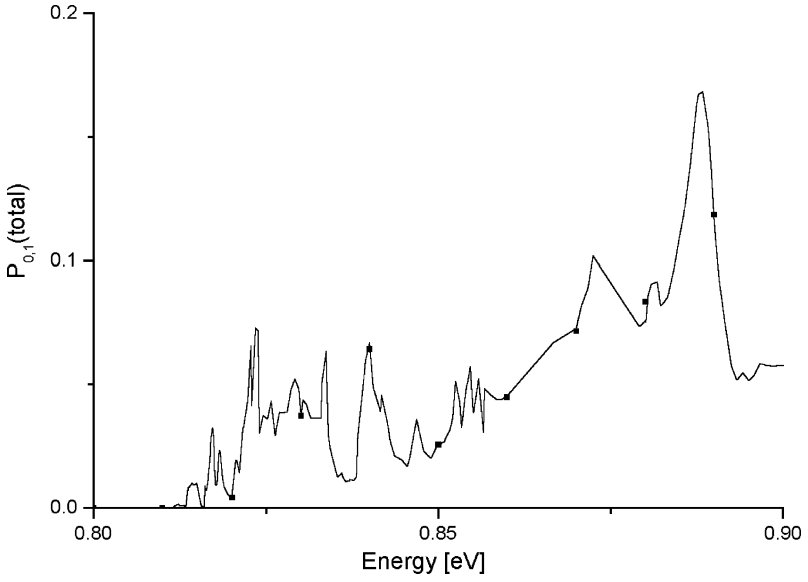

(b)

Fig. 8. The same as Figs. 7 for the reaction probability from the ground ro-vibrational state of O_2 summed over the product quantum states.

30 a.u., $N_{sct} = 141$, $N_\rho = 8$. The size of one sector was chosen to be approximately the local wavelength at the maximum energy considered and actually ranges from $\sim$0.14 a.u. at small ρ to $\sim$0.21 a.u. in the asymptotic region.

The results of the calculations are depicted in Figs. 7 and 8. Figs. 7 represent the total cumulative reaction probability $N(E)$. We show (a) the full energy interval and (b) magnification of the low energy portion near the

region of $E \simeq 0.818$ eV. Figs. 8 represent the data in the same energy intervals for the reaction probability from the ground state ($v_i = 0,\ j_i = 1$) of O_2 summed over all ro-vibrational states in the final O + HO channel. In all the figures the total energy E is measured in eV from the ground state ($v_i = 0,\ j_i = 1$) of $O_2(0, 1)$ and the solid line corresponds to the results with the parameters given above. To provide a convergence test we improved the accuracy of the surface functions by using larger n_{ad} and repeated the calculations. The number of the propagated channels were increased up to 350 in the condensation and 290 in the asymptotic region. In Figs. 7 and 8 the improved results are shown by squares. These two sets of results show good agreement. The symmetry of the S-matrix at energies below 1.05 eV is satisfied up to 5 significant digits or better. Even at the highest energy it is not worse than 3 digits and at most of the points 4 digits. At energies $E > 1.3$ eV some discrepancies can be seen. Note, however, that the number of calculated points is obviously not enough to fully resolve the resonance structure of scattering data. The heavy resonances prevent us from a direct comparison with the previous results obtained with use of the log derivative method [33], although visually they are the same. In particular we cannot be absolutely sure whether the subroutines for PES were completely identical. Clearly, in the vicinity of the resonances even a small disagreement in PES may lead to noticeable difference in the calculated probability. However, from the convergence test given in [33] and the comparison of our results obtained with two different sets of parameters we can judge that the accuracy of our data is similar. Since the number of the propagated channels and the matching radius are also the same as in previous calculations, the following analysis can be made. The calculations of Pack et al. required at one energy 7339 symmetric matrix inversions and 444 matrix multiplications [33]. In our program the number of matrix operations for each of 141 sectors is determined as follows:

(i) The evaluation of two symmetric and one rectangular sector R-matrices which amounts to $2\,N_\rho \frac{N_d}{N_{ch}} \frac{3}{4} + 1\,N_\rho \frac{N_d}{N_{ch}} \frac{3}{2}\ N_{ch}^3$ operations;

(ii) The propagation itself (Eq. (7)) which in the Nesbet algorithm is equivalent to $1.5\,N_{ch}^3$ operations, giving totally 4089 N_{ch}^3 operations. This is about twice less in cpu time. The actual cpu time can be further decreased by reducing N_{ch} in the asymptotic region. More extended analysis of the results and the discussion about the reaction mechanisms are beyond the scope of this paper and will be reported elsewhere.

4. Conclusion

In the present work we have proposed a new method of time-independent scattering calculation which combines the advantages of diabatic-by-sector [4] and the TN (Tolstikhin–Nakamura) adiabatic-by-sector [1] approaches. Similar to Ref. [1] we implemented the R-matrix propagation recipe of Baluja et al. [8], but the sector R-matrices are calculated in a different way. The adiabatic surface functions at the boundaries of each sector are taken as a variational basis and used to evaluate all the necessary quantities for energy dependent part of the calculation. Thus we do not need to consider the adiabatic eigenvalue problem at many other intermediate values of the scattering coordinate, which can reduce the volume of computation considerably. There are several other improvements related with this modification. The new scheme provides a very natural and easy way for changing the number of the propagated channels N_{ch}. For systems with deep potential well in the condensation region this gives an additional resource for reducing the cpu time. Besides, the new scheme requires the computation of only one overlap matrix per sector. This makes any method of solving the surface function equation feasible. We have not yet implemented this option. Among the existing DBS codes the most appropriate one is the method by Schneider and Walker [12] which utilizes the similar technique of R-matrix propagation. The present code can be formally modified from the code of Schneider and Walker, if we change the definition of the R-matrix (and also sector R-matrices) and use the set of DVR basis functions for the radial motion. The choice of the surface functions is also different and enables us to avoid any fitting and matching procedures. We have shown that the accuracy of the results can be significantly improved by a small increase of their number.

We have illustrated the method by taking two chemical reactions, O + HCl and H + O_2, and found it to be very effective. In particular in the OHCl case the present calculations are found to be 8 times less expensive than those

in [1] simply because of the reduction of the number of diagonalization on the hypersphere. The method is easy to program and it is effective especially when the density of adiabatic levels is large like in the presently studied HO_2 system. In energy dependent part of the calculations the main part of the cpu time is spent to compute the sector matrices Eq. (8). Therefore at higher collision energies the present method might become slower than the DBS method due to the increasing dimension of R-matrix basis. Hopefully, this can be remedied by truncating the spectral representation in Eq. (8) based on the Buttle correction [43,44].

Acknowledgements

G.V.M. is thankful for the support of the Japan Society for the Promotion of Science during his stay at IMS as a JSPS fellow. This work was partially supported by the Grant-in-Aid for Scientific Research on Priority Area "Molecular Physical Chemistry" and by the Research Grant No.10440179 from the Ministry of Education, Science, Culture and Sports of Japan.

References

[1] O.I. Tolstikhin, H. Nakamura, J. Chem. Phys. 108 (1998) 8899.
[2] O.I. Tolstikhin, S. Watanabe, M. Matsuzawa, J. Phys. B 29 (1996) L389.
[3] J.C. Light, Z. Bacic, J. Chem. Phys. 87 (1987) 4008.
[4] J.C. Light, R.B. Walker, J. Chem. Phys. 65 (1976) 4272.
[5] L.D. Thomas, M.H. Alexander, B.R. Johnson, W.A. Lester Jr., J.C. Light, K.D. McLenithan, G.A. Parker, M.J. Redmon, T.G. Schmalz, D. Secrest, R.B. Walker, J. Comp. Phys. 41 (1981) 407.
[6] K. Hino, A. Igarashi, J.H. Macek, Phys. Rev. A 56 (1997) 1038.
[7] A. Igarashi, N. Toshima, T. Shirai, Phys. Rev. A 50 (1994) 4951.
[8] K.L. Baluja, P.G. Burke, L.A. Morgan, Comput. Phys. Commun. 27 (1982) 299.
[9] R.M. Whitnell, J.C. Light, J. Chem. Phys. 90 (1989) 1774.
[10] K. Nobusada, O.I. Tolstikhin, H. Nakamura, J. Mol. Str. (THEOCHEM) 461–462 (1999) 137–144.
[11] G.V. Mil'nikov, O.I. Tolstikhin, K. Nobusada, H. Nakamura, Phys. Chem. Chem. Phys. 1 (1999) 1159.
[12] B.I. Schneider, R.B. Walker, J. Chem. Phys. 70 (1979) 2466.
[13] S.E. Choi, J.C. Light, J. Chem. Phys. 97 (1992) 7031.
[14] T.N. Rescigno, C.W. McCurdy, Phys. Rev. A 31 (1985) 624.
[15] W.H. Miller, B.M.D.D. Jansen op de Haar, J. Chem. Phys. 86 (1987) 6213.
[16] R.K. Nesbet, J. Comp. Phys. 8 (1971) 483.
[17] A. Persky, M. Broida, J. Chem. Phys. 81 (1984) 4352.
[18] O.I. Tolstikhin, S. Watanabe, M. Matsuzawa, Phys. Rev. Lett. 74 (1995) 3573.
[19] K. Bathe, E.L. Wilson, Numerical Methods in Finite Element Analysis, Prentice Hall, New York, 1976.
[20] J.M. Launau, M. LeDourneuf, Chem. Phys. Lett. 169 (1990) 473.
[21] L. Wolniewicz, J. Chem. Phys. 90 (1989) 371.
[22] G.A. Parker, R.T. Park, J. Chem. Phys. 98 (1993) 6883.
[23] A.J.C. Varandas, J. Chem. Phys. 99 (1993) 1076.
[24] D.A. Masten, R.K. Hanson, C.T. Bowman, J. Phys. Chem. 94 (1990) 7119.
[25] K.S. Shin, J.V. Michael, J. Chem. Phys. 95 (1991) 262.
[26] H. Du, J.P. Hessler, J. Chem. Phys. 96 (1992) 1077.
[27] K. Kesler, K. Kleinermanns, J. Chem. Phys. 97 (1992) 374.
[28] J.A. Miller, R.J. Kee, C.K. Westbrook, Annu. Rev. Phys. Chem. 41 (1990) 345, and references therein.
[29] D.H. Zhang, J.Z.H. Zhang, J. Chem. Phys. 101 (1994) 3671.
[30] E.M. Goldfield, A.J.H. Meijer, J. Chem. Phys. 113 (2000) 11 055.
[31] L.B. Harding, A.I. Maergoiz, J. Troe, V.G. Ushakov, J. Chem. Phys. 113 (2000) 11 019.
[32] R.T. Pack, E.A. Butcher, G.A. Parker, J. Chem. Phys. 99 (1993) 9310.
[33] R.T. Pack, E.A. Butcher, G.A. Parker, J. Chem. Phys. 102 (1995) 5998.
[34] A. Ohsaki, H. Nakamura, Physics Reports 187 (1990) 1.
[35] V. Aquilanti, in: D.C. Clary (Ed.), The Theory of Chemical Reaction Dynamics, Reidel, Dordrecht, 1986, p. 383.

[36] K. Nobusada, O.I. Tolstikhin, H. Nakamura, J. Chem. Phys. 108 (1998) 8922; J. Phys. Chem. A 102 (1998) 9445.
[37] U. Fano, Phys. Rev. A. 24 (1981) 2402; Rep. Prog. Phys. 46 (1983) 97.
[38] M.R. Pastrana, L.A.M. Quintales, J. Brandão, A.J.C. Varandas, J. Phys. Chem. 94 (1990) 8073.
[39] W.H. Miller, J. Chem. Phys. 629 (1975) 189.
[40] W.H. Miller, S.D. Schwartz, J. Tromp, J. Chem. Phys. 79 (1983) 4889.
[41] T. Seideman, W.H. Miller, J. Chem. Phys. 96 (1992) 4412; 97 (1992) 2499.
[42] O.I. Tolstikhin, V.N. Ostrovsky, H. Nakamura, Phys. Rev. Lett. 80 (1998) 41.
[43] P.J.A. Buttle, Phys. Rev. 160 (1967) 719.
[44] D.J. Zvijac, J.C. Light, Chem. Phys. 12 (1976) 237.